Cell Reports

Report

Differential cell-cycle control by oscillatory versus sustained Hes1 expression via p21

Graphical abstract

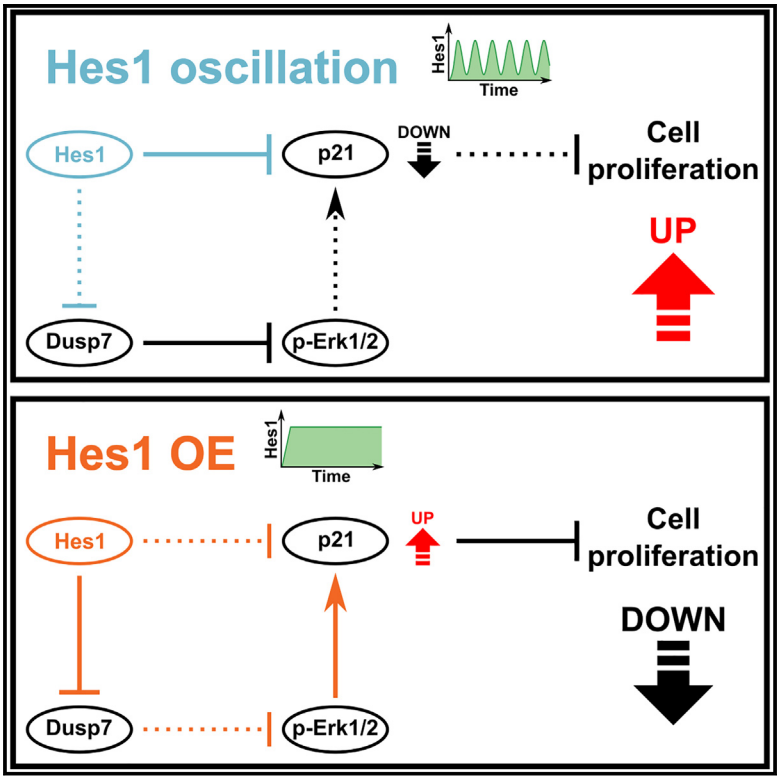

Highlights

- Oscillatory Hes1 activates neural stem cell proliferation by repressing p21
- High and sustained Hes1 inhibits neural stem cell proliferation by inducing p21
- High and sustained Hes1 increases phosphorylated Erk, which induces p21

Authors

Yuki Maeda, Akihiro Isomura, Taimu Masaki, Ryoichiro Kageyama

Correspondence

ryoichiro.kageyama@riken.jp

In brief

Maeda et al. show that the transcription factor Hes1 activates or inhibits proliferation of neural stem cells by changing its expression patterns to be oscillatory or high and sustained, respectively. The cyclin-dependent kinase inhibitor p21, which delays cell-cycle progression, is repressed by oscillatory Hes1 but up-regulated by high and sustained Hes1.

Maeda et al., 2023, Cell Reports *42*, 112520
May 30, 2023
https://doi.org/10.1016/j.celrep.2023.112520

CellPress

Cell Reports

CellPress
OPEN ACCESS

Report

Differential cell-cycle control by oscillatory versus sustained Hes1 expression via p21

Yuki Maeda,[1,2] Akihiro Isomura,[3,4,5] Taimu Masaki,[1] and Ryoichiro Kageyama[1,2,6,7,*]
[1]RIKEN Center for Brain Science, Wako 351-0198, Japan
[2]Graduate School of Biostudies, Kyoto University, Kyoto 606-8501, Japan
[3]Institute for Life and Medical Sciences, Kyoto University, Kyoto 606-8507, Japan
[4]Institute for Integrated Cell-Material Sciences, Kyoto University, Kyoto 606-8501, Japan
[5]Japan Science and Technology Agency, PRESTO, Saitama 332-0012, Japan
[6]Graduate School of Medicine, Kyoto University, Kyoto 606-8501, Japan
[7]Lead contact
*Correspondence: ryoichiro.kageyama@riken.jp
https://doi.org/10.1016/j.celrep.2023.112520

SUMMARY

Oscillatory Hes1 expression activates cell proliferation, while high and sustained Hes1 expression induces quiescence, but the mechanism by which Hes1 differentially controls cell proliferation depending on its expression dynamics is unclear. Here, we show that oscillatory Hes1 expression down-regulates the expression of the cyclin-dependent kinase inhibitor p21 (Cdkn1a), which delays cell-cycle progression, and thereby activates the proliferation of mouse neural stem cells (NSCs). By contrast, sustained *Hes1* overexpression up-regulates p21 expression and inhibits NSC proliferation, although it initially down-regulates p21 expression. Compared with Hes1 oscillation, sustained Hes1 overexpression represses Dusp7, a phosphatase for phosphorylated Erk (p-Erk), and increases the levels of p-Erk, which can up-regulate p21 expression. These results indicate that p21 expression is directly repressed by oscillatory Hes1 expression, but indirectly up-regulated by sustained Hes1 overexpression, suggesting that depending on its expression dynamics, Hes1 differentially controls NSC proliferation via p21.

INTRODUCTION

Embryonic neural stem cells (NSCs) proliferate actively, while adult NSCs are mostly quiescent and occasionally become activated to undergo proliferation.[1] The detailed mechanism by which the active and quiescent states of NSCs are controlled remains to be analyzed. It has been shown that the Notch signaling pathway plays an important role in the active and quiescent states of NSCs: Notch1 signaling is required for the maintenance of proliferating NSCs, whereas Notch2 signaling induces quiescence in NSCs.[2–7] The Notch signaling effector Hes1, a transcriptional repressor, is also required for both active and quiescent NSCs in the adult and embryonic brain.[8] Interestingly, Hes1 shows distinct expression patterns between active and quiescent NSCs: its expression is oscillatory in proliferating NSCs but is much higher and sustained in quiescent NSCs.[8,9] These results suggest that the oscillatory versus high and sustained expression of Hes1 is important for the active versus quiescent state of NSCs. Indeed, when Hes1 oscillations are dampened by genetic manipulation, NSC proliferation is impaired, leading to microcephaly.[10,11] Furthermore, cells in the boundary regions such as the isthmus, which demarcates the border between the midbrain and hindbrain, and the roof and floor plates, which demarcate the borders between the right and left halves of the neural tube, are quiescent and non-neurogenic and express constantly high levels of Hes1, but when *Hes1* and its related genes are knocked out, the features of boundary cells are lost.[12,13] Thus, the expression dynamics of Hes1 are important for the active and quiescent states of NSCs, but the detailed downstream mechanism by which oscillatory and sustained Hes1 expression differentially control NSC proliferation remains to be analyzed.

High Hes1 expression inhibits cell-cycle progression not only in NSCs but also in other cell types such as fibroblasts and progenitor cells.[13,14] For example, serum deprivation or contact inhibition can lead to high levels of Hes1 and a quiescent state in fibroblasts and preadipocytes.[15,16] It was also shown that Hes1 is expressed at high levels in quiescent hematopoietic stem/progenitor cells and quiescent muscle satellite cells,[17,18] while Hes1 expression oscillates in activated muscle stem cells.[19] Interestingly, quiescent human fibroblasts lose their ability to resume proliferation and enter senescence when *Hes1* is knocked down, whereas high and sustained Hes1 expression is sufficient to prevent these cells from entering senescence associated with prolonged cell cycle arrest.[15] Thus, high and sustained Hes1 expression may reversibly inhibit cell-cycle progression in many cell types, including NSCs.

Here, we examined the significance of Hes1 expression dynamics in the proliferation of NSCs and found that oscillatory versus sustained Hes1 expression differentially controls the

cyclin-dependent kinase (CDK) inhibitor p21 (Cdkn1a). p21 is known to have dual activities in cell-cycle progression depending on its expression levels[20]: high levels of p21 inhibit the activity of CDK4/cyclin D1 complexes, thereby inducing cell cycle arrest, whereas low p21 levels promote the assembly of active CDK4/cyclin D1 complexes, which drive cell proliferation.[21] We found that p21 expression is down-regulated by oscillatory Hes1 expression, leading to activation of NSC proliferation, whereas it is up-regulated by high and sustained Hes1 expression, leading to inhibition of NSC proliferation. We further examined the mechanism by which Hes1 differentially controls p21 expression in NSCs.

RESULTS

Differential cell-cycle control by oscillatory or overexpressed Hes1 in NSCs

We first examined Hes1 expression patterns in proliferating mouse NSCs using a fluorescent ubiquitination-based cell-cycle indicator (FUCCI) probe, which can monitor the phases of the cell cycle.[22] To this end, we used mouse embryonic stem cell-derived NSCs (NS5 cells)[23] that carried the destabilized firefly luciferase (Luc2) under the control of the *Hes1* promoter to monitor *Hes1* promoter activity.[24] *Hes1* expression was examined by bioluminescence exerted from these NSCs cultured in the presence of luciferin. Live-imaging analyses showed that *Hes1* expression oscillated with a periodicity of 2–3 h throughout the cell cycle (Figures 1A, 1B, and S1A). One of the features of the relationship between *Hes1* oscillations and the phases of the cell cycle was that most cells exhibited a trough phase of expression followed by a peak phase after cell division (Figures 1C and 1D, left panels). This is probably due to transcriptional reactivation at mitotic exit.[25,26] While the first peak and second trough were clear, the second peak was less pronounced (Figures 1C and 1D, left panels), suggesting that *Hes1* oscillations soon desynchronize between NSCs. Another feature was that a trough phase followed by a peak phase appeared frequently during the G1/S transition (Figures 1C and 1D, right panels). Human breast cancer cells also reportedly exhibit a Hes1 trough phase at the G1/S transition,[27] suggesting that it is a common feature among dividing cells.

We next examined the requirement for *Hes1* in the proliferation of NSCs, which was monitored by EdU incorporation. When Hes1 was knocked down, proliferation of NS5 cells was not significantly affected (Figure S1B). Similarly, proliferation of embryonic NSCs (eNSCs) was not significantly affected when *Hes1* was knocked out because the functions of Hes1 can be compensated for by its family members such as Hes3 and Hes5.[8,28] In the absence of *Hes3*, *Hes5*, and *Hey1*, EdU incorporation was reduced in eNSCs, and it was reduced further when *Hes1* was additionally knocked out, suggesting that *Hes1*, *Hes3*, *Hes5*, and *Hey1* cooperatively activate NSC proliferation (Figure 1E), as observed previously *in vivo*.[8]

We next induced the continuous overexpression of *Hes1* in NSCs (both NS5 and eNSCs) using the Tet-ON system (Figure 1F), which continuously up-regulated Hes1 expression after administration of doxycycline (Figure S1C). Hes1 induction by a low dosage of doxycycline reduced EdU incorporation slightly, while higher dosages significantly reduced EdU incorporation and increased G1 and G2 phases, suggesting that both G1 and G2 phases are delayed by Hes1 overexpression (Figures 1F, S1E, and S1F). Doxycycline administration alone did not affect EdU incorporation of NSCs (Figure S1D). These results indicated that NSC proliferation is inhibited by sustained *Hes1* overexpression. Thus, both *Hes* gene inactivation and sustained *Hes1* overexpression reduced EdU incorporation compared with wild-type NSCs, in which *Hes1* expression oscillates, suggesting that *Hes1* oscillations are required for efficient proliferation of NSCs.

Hes1 overexpression-induced cell-cycle inhibition by p21

To understand the mechanism by which Hes1 differentially regulates NSC proliferation depending on its expression patterns, we performed RNA sequencing (RNA-seq) analyses comparing between wild-type eNSCs and *Hes1;Hes3;Hes5;Hey1* knockout (KO) eNSCs and between wild-type and *Hes1*-overexpressing NS5 cells (Figure 2A; Tables S1 and S2). Among the genes involved in cell-cycle regulation, mRNAs of the CDK inhibitors $p15^{INK4b}$ (Cdkn2b) and p21 (Cdkn1a), which delay or stop cell-cycle progression by inhibiting CDK activity, were up-regulated in *Hes1;Hes3;Hes5;Hey1* KO eNSCs and *Hes1*-overexpressing NS5 cells compared with wild-type NSCs, in which Hes1 expression oscillates (Figure 2B; Table S3). Particularly, p21 protein was significantly up-regulated when *Hes1* was overexpressed compared with wild-type NSCs (Figure 2C), while $p15^{INK4b}$ protein was undetectable in these cells (Figure 2C). These results suggest that p21 is mainly responsible for the Hes1-overexpression-induced inhibition of NSC proliferation. To examine this notion, we knocked down p21 expression in *Hes1*-overexpressing NS5 cells and found that EdU incorporation was partially recovered (Figure 2D). These results indicated that Hes1 overexpression inhibits the proliferation of NSCs by up-regulating p21 expression. p21 knockdown in wild-type NS5 cells did not make any significant changes but showed a weak tendency to reduce EdU uptake (Figure S1G), suggesting that certain levels of p21 expression are required for efficient proliferation of NSCs.

To examine whether high and sustained expression of Hes1 is involved in p21 expression in the developing nervous system, we examined the isthmus, whose cells are quiescent and express high levels of p21.[29] In this region, *Hes1* and *Hes3* are expressed steadily at high levels.[12] In *Hes3;Hes5* double KO mice, p21 is expressed normally in the isthmus (Figure 2E, arrowheads), but when *Hes1* was additionally knocked out, p21 expression was severely down-regulated (Figure 2E). These results indicated that steady high levels of Hes1 expression are responsible for p21 expression in the isthmus.

Differential control of p21 expression by oscillatory or overexpressed Hes1

We next examined whether p21 expression is differentially controlled by oscillatory or sustained expression of Hes1 in NS5 cells. A p21 promoter-driven destabilized luciferase reporter (p21-luc), which can monitor transcription from the p21 promoter, was introduced into NS5 cells. Hes1 oscillations were induced by the optogenetic hGAVPO system, in which

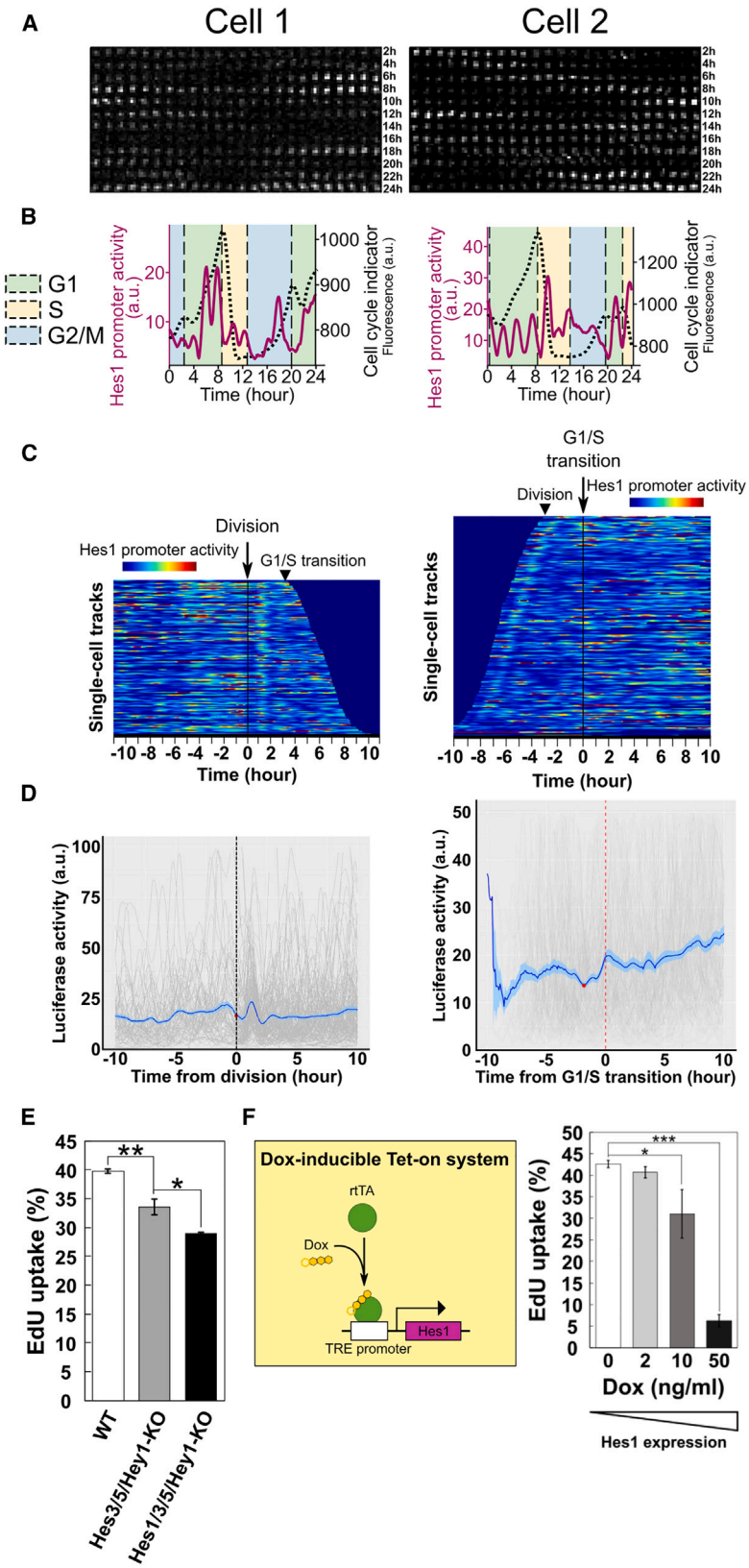

Figure 1. Differential control of NSC proliferation depending on Hes1 expression dynamics

(A and B) Single-cell bioluminescence imaging of Hes1 expression with cell-cycle phase in proliferating NSCs. Representative images (A) and quantification of Hes1 expression (purple solid line) and a cell-cycle indicator (black dotted line) (B). Background colors in graphs indicate the cell-cycle phases (G1 phase, green; S phase yellow; G2/M phase, blue).

(C) Heatmap of Hes1 expression. (Left) Cell division was set at time 0. n = 133 cells. (Right) The G1-S transition was set at time 0. n = 209 cells.

(D) Hes1 expression of each cell. Gray and blue lines and blue-shaded area indicate single-cell signals, mean values, and standard errors, respectively. The black and red dotted lines indicate cell division (left) and G1-S transition (right), respectively.

(E) EdU incorporation of wild-type (WT; control), *Hes3*;*Hes5*;*Hey1*-KO, and *Hes1*;*Hes3*;*Hes5*;*Hey1*-KO eNSCs. n = 3 independent experiments.

(F) EdU incorporation of *Hes1*-overexpressing NSCs. *Hes1* expression was induced by the Tet-ON system (left) with 0, 2, 10, or 50 ng/mL doxycycline (Dox). n = 3 independent experiments.

Data represent means ± SEM (*p < 0.05, **p < 0.01, ***p < 0.001; Student's t test).

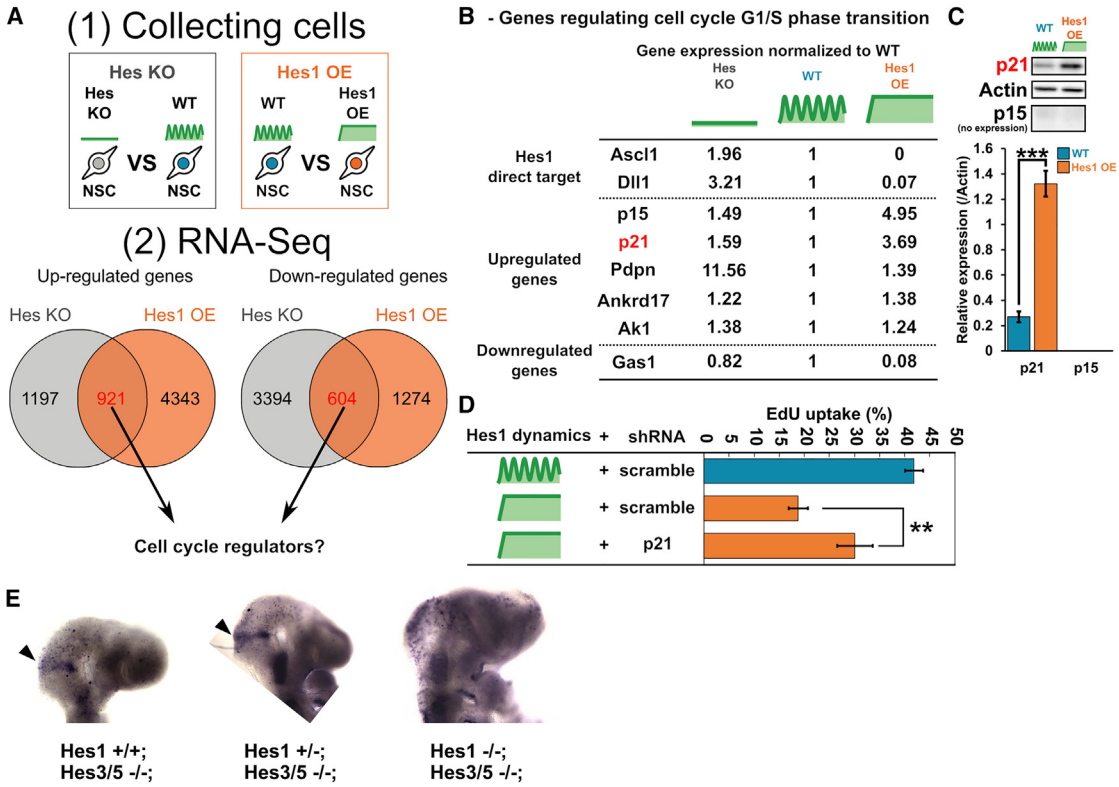

Figure 2. Up-regulation of p21 expression in Hes1-overexpressing quiescent/slowly dividing cells

(A) RNA-seq analyses of WT, *Hes1*;*Hes3*;*Hes5;Hey1*-KO (Hes KO), and *Hes1*-overexpressing (OE) NSCs.

(B) Fold changes of gene expression. Up-regulated or down-regulated genes in Hes KO and *Hes1*-OE NSCs were selected. n = 3 independent experiments.

(C) Expressions of p21 and p15 proteins in WT and *Hes1*-OE NSCs. n = 3 independent experiments. See the raw data in Figure S4.

(D) EdU incorporation of WT NSCs with scrambled RNA and *Hes1*-OE NSCs with scrambled RNA or p21 shRNA. n = 3 independent experiments.

(E) Whole-mount *in situ* hybridization of p21 in the isthmus (arrowheads) of *Hes3*;*Hes5*-null (n = 2 embryos), *Hes1*(+/−);*Hes3*;*Hes5*-null (n = 2 embryos), and *Hes1;Hes3*;*Hes5-null* (n = 3 embryos) mice at E9.5.

Data represent means ± SEM (**p < 0.01, ***p < 0.001; Student's t test).

Hes1 expression can be induced by blue light illumination but suppressed under dark conditions (Figure 3A).[9,24] When Hes1 oscillations were induced by this optogenetic method, endogenous Hes1 expression also oscillated synchronously with the exogenous Hes1 oscillations at the population level.[24] Under this condition, p21 transcription was down-regulated after each Hes1 pulse, resulting in oscillations at the population level (Figure 3B, orange line), suggesting that Hes1 oscillations drive p21 oscillations by periodic repression. p21 expression reportedly exhibits oscillations in response to DNA damage under the control of p53, which also shows pulsatile expression.[30] However, the expression dynamics of p21 in proliferating NSCs have not been characterized. Therefore, we next examined p21 expression in active NS5 cells using the p21-luc along with the FUCCI probe. Time-lapse imaging analysis revealed that p21 transcription oscillated with a periodicity of ~3 h in proliferating NS5 cells (Figures 3C, 3D, and S2A). These results suggest that Hes1 oscillations periodically repress p21 transcription, thereby driving p21 oscillations. p21 expression exhibited a trough phase followed by a peak phase after cell division (Figure 3D). Interestingly, p21 expression was down-regulated at the G1/S transition (Figure 3E), as reported previously,[31,32] when Hes1 exhibited a peak phase of expression (see Figure 1D, right panel), supporting the notion that Hes1 oscillations repress p21 expression. We also examined p21 protein expression in proliferating NSCs by knocking in the Achilles fluorescent reporter[33] into the p21 locus so that p21-Achilles fusion protein is expressed from the p21 locus (Figure S2B). Time-lapse imaging analysis showed that p21 protein expression did not oscillate with a ~3-h periodicity but changed according to the phase of the cell cycle (Figures 3F and S2C). The p21-Achilles fusion protein (half-life = ~161.4 min) was more stable than the intact p21 protein (half-life = ~39 min) (Figure S2D), which may explain why oscillation with a ~3-h periodicity was not detectable. Nevertheless, p21-Achilles fusion protein expression was dynamic: up-regulated during the G1 phase but repressed about 1 h after the G1-S transition (Figures 3F and S2C). The repression of p21-Achilles fusion protein expression was delayed compared with p21 transcription, probably because this fusion protein is stable, suggesting that the intact p21 protein expression is repressed around the G1-S transition.

We next examined the effect of sustained Hes1 overexpression on p21 expression. When Hes1 overexpression was induced by the Tet-ON system, p21 expression was initially

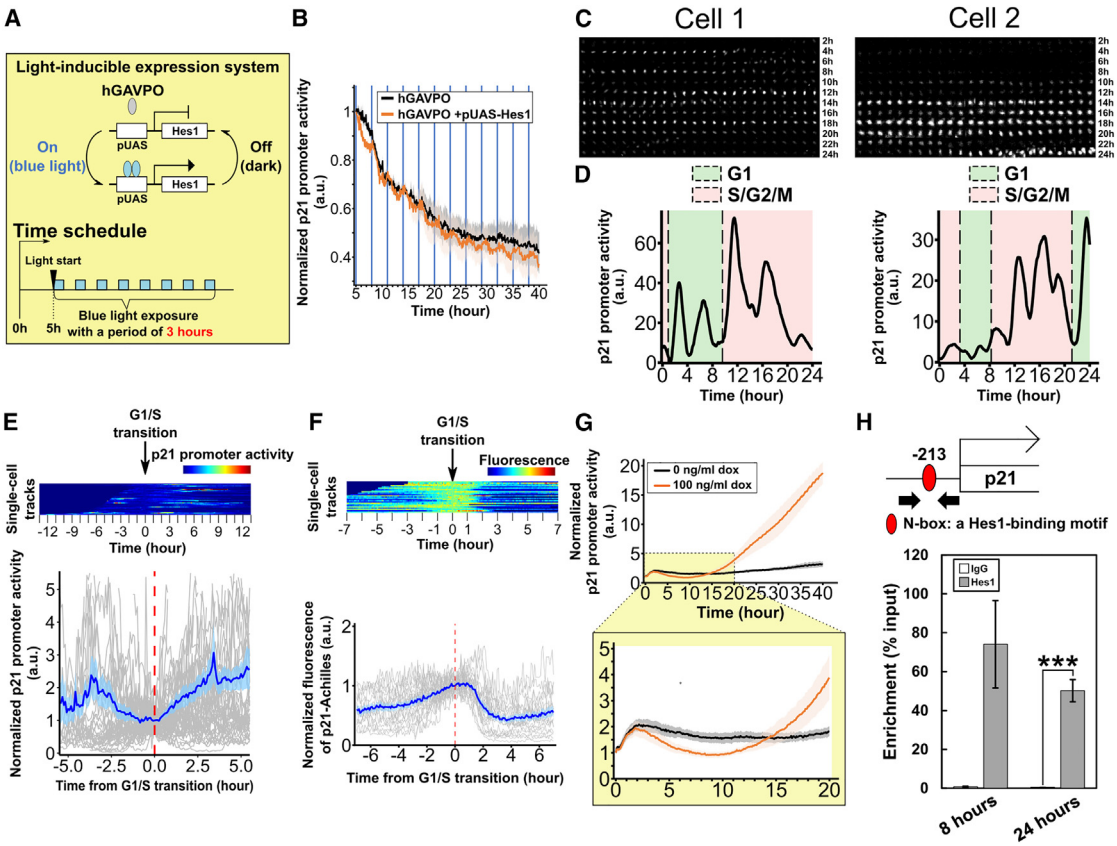

Figure 3. Differential control of p21 expression by oscillatory or overexpressed Hes1

(A) (Top) Schematic of the light-inducible expression system using hGAVPO. (Bottom) Time schedule of light stimulation. The medium was changed from growth medium to quiescent medium just before starting live-cell monitoring.

(B) p21 expression in NSCs under the control of oscillatory Hes1 expression (hGAVPO + pUAS-Hes1) or no exogenous Hes1 (hGAVPO). n = 3 independent experiments.

(C and D) Single-cell bioluminescence imaging of p21 expression with cell-cycle phase in proliferating NSCs. Representative images (C) and quantification of p21 expression (D). Background colors indicate cell-cycle phases (G1 phase, green; S/G2/M phase, pink).

(E) (Top) Heatmap of p21 promoter activity. G1/S transition was set at time 0 (red dotted line). (Bottom) p21 expression in NSCs. Gray and blue lines and blue-shaded area indicate single-cell signals, mean values, and standard errors, respectively. n = 46 cells.

(F) Heatmap of p21 protein expression in proliferating NSCs. G1/S transition was set at time 0 (red dotted line). n = 25 cells.

(G) p21 expression in NSCs under the control of sustained *Hes1* overexpression (100 ng/mL Dox) or no exogenous Hes1 (0 ng/mL Dox) by the Tet-ON system. Shaded areas indicate standard errors. The bottom graph is a magnified image of the top graph. n = 5 independent experiments.

(H) Chromatin immunoprecipitation qPCR with an anti-Hes1 antibody or control immunoglobulin G (IgG) on the p21 promoter. Chromatin was isolated from NSCs 8 and 24 h after *Hes1* overexpression induced by the Tet-ON system with 100 ng/mL Dox. qPCR analysis was performed with primers for the binding sites shown in the schematic. n = 3 independent experiments.

Data represent means ± SEM (***p < 0.001; Student's t test).

down-regulated (Figure 3G, bottom panel, orange line), but ~10 h later, its expression began to increase and continued to be up-regulated (Figure 3G, top panel, orange line). As a negative control, doxycycline administration alone did not affect p21 expression in NS5 cells (Figure S2E). These results suggest that Hes1 overexpression can down-regulate p21 expression initially, but this effect is reversed when its expression is maintained over a certain period of time. Chromatin immunoprecipitation (ChIP) analysis using an anti-Hes1 antibody showed that Hes1 protein physically interacted with the p21 promoter region at both 8 and 24 h after doxycycline administration (Figure 3H). As Hes1 is a transcriptional repressor,[34] it is likely that Hes1 can repress p21 expression by binding directly to its promoter and that continuous Hes1 overexpression leads to delayed p21 up-regulation by an indirect pathway.

Involvement of the MEK-Erk pathway in Hes1 overexpression-induced p21 up-regulation

To identify the mechanism by which sustained Hes1 overexpression can up-regulate p21 expression, we next tested the possibility that Hes1 may function as a transcriptional activator of p21. Calcium/calmodulin-dependent protein kinase 2δ (CaMK2δ) can reportedly switch Hes1 from a transcriptional repressor to a transcriptional activator by phosphorylation.[35,36] However, treatment with the CaMK2δ inhibitor KN-62 did not show any significant effects on the Hes1-dependent induction

of p21 expression (Figure S2F), suggesting that the CaMK2δ-dependent switch of Hes1 function is not involved in the induction of p21 expression.

We next compared other signaling molecules between control and *Hes1*-overexpressing NS5 cells. We found that phosphorylated Stat3 (p-Stat3) and p-Erk1/2 levels were increased by Hes1 overexpression (Figure 4A). To investigate the functional requirement for each signaling molecule, we examined the effects of MEK and JAK inhibitors on p21 expression. While the JAK inhibitor AG490 did not make any significant changes, the MEK inhibitor PD0325901 significantly repressed p21 expression in *Hes1*-overexpressing NSCs (Figure 4B). Furthermore, PD0325901 administration partially recovered EdU incorporation in *Hes1*-overexpressing NSCs (Figure 4C). These results suggest that activation of Erk1/2 signaling is responsible for p21 up-regulation by Hes1 overexpression. PD0325901 administration reduced both p21 expression and EdU uptake in wild-type NS5 cells (Figures 4B and 4C), suggesting that certain levels of p-Erk1/2 and p21 expression are required for efficient proliferation of NSCs. Interestingly, inhibition of Erk signaling reduced p21 expression to approximately the same levels in wild-type and Hes1-overexpressing NS5 cells (Figure 4B), and this was associated with EdU uptake approaching equal levels in the two systems (Figure 4C), suggesting that increasing p21 levels slightly above this level leads to cell proliferation whereas increasing p21 levels by a large amount inhibits the cell cycle.

It was previously reported that p-Erk1/2 levels are oscillating in proliferating cells and that their frequency is important for efficient cell proliferation.[37,38] Furthermore, constitutive overactivation of p-Erk1/2 levels leads to up-regulation of p21 and cell cycle arrest.[39,40] We therefore examined Erk activity in NS5 cells using the Erk kinase translocation reporter, which detects fluctuation in Erk activity at a single-cell resolution.[41] Live-imaging analysis showed that Erk activity fluctuated at lower levels with some spikes in wild-type NS5 cells whereas it was up-regulated in Hes1-overexpressing NS5 cells (Figures S3A–S3C). These results raised the possibility that Hes1 overexpression leads to more continuous activation of Erk1/2 signaling, thereby up-regulating p21 expression.

We next examined the mechanism by which Hes1 overexpression increased Erk1/2 phosphorylation. As Erk1/2 protein levels were not much changed by Hes1 overexpression (Figure 4A), kinase and/or phosphatase levels may be changed. Indeed, RNA-seq analysis indicated that the expression of Dusp7, a phosphatase of p-Erk1/2, was suppressed by Hes1 overexpression in NSCs (Figure 4D; Table S2). Western blot analysis showed that the Dusp7 protein was down-regulated by Hes1 overexpression in NSCs (Figure 4D). Furthermore, Dusp7 overexpression decreased p-Erk1/2 and p21 levels (Figure S3D) and partially rescued EdU incorporation in *Hes1*-overexpressing NSCs (Figure 4E). ChIP analysis showed that the Hes1 protein binds to the regulatory sequence in the Dusp7 gene (Figure 4F). These results suggest that sustained Hes1 overexpression leads to the suppression of Dusp7 by binding to its regulatory sequence and to a resultant increase of p-Erk1/2 levels, which induce the delayed up-regulation of p21 expression and inhibition of NSC proliferation.

DISCUSSION

Here, we found that depending on its expression dynamics, Hes1 can differentially control NSC proliferation via p21. Recent analysis indicated that persistent Hes1 expression at low to intermediate levels does not inhibit the proliferation of NSCs but does impede the reactivation of quiescent NSCs.[42] We also found that NSC proliferation was inhibited only weakly by low levels of sustained Hes1 expression, but was strongly inhibited by high Hes1 expression levels, suggesting that not only sustained versus oscillatory expression but also expression levels of Hes1 are important to inhibit cell proliferation.

In active NSCs, Hes1 oscillations periodically repress the proneural gene *Ascl1*, inducing *Ascl1* oscillations, whereas in quiescent NSCs, Hes1 expression is higher and continuously suppresses *Ascl1* expression.[8] *Ascl1* has been shown to have dual activities: activation of NSC proliferation and induction of cell-cycle exit and subsequent neuronal differentiation.[43] Indeed, *Ascl1* exhibits such dual actions depending on its expression patterns: *Ascl1* induces neuronal differentiation when its expression is sustained, whereas it activates NSC proliferation when its expression is oscillatory.[9] Thus, when Ascl1 is continuously repressed, NSC proliferation is inhibited. Interestingly, genes involved in cell-cycle progression such as Cdk1 and E2f1 are up-regulated by Asc1l[44] but repressed by Hes1 overexpression (Tables S1 and S2). Thus, high and sustained Hes1 expression antagonizes Ascl1 and its target cell-cycle activators, leading to NSC quiescence.

Human breast cancer cells exhibit Hes1 oscillations with a periodicity of ~25 h in addition to ultradian rhythms.[27] In these cells, the G1/S transition occurs during the Hes1 dip, which is similar to our results with mouse NSCs. However, mitosis of these cancer cells occurs mostly during the Hes1 peak, which is different from NSCs. Our previous results suggest that Hes1 protein expression is mostly negative near the ventricular surface of the developing nervous system,[45] where mitosis occurs, suggesting that most NSCs undergo mitosis during the Hes1 dip. Thus, only the Hes1 dip during the G1/S transition seems to be a common feature observed in different types of dividing cells.

The finding of a single factor exhibiting different activities depending on its expression patterns is also observed in other systems.[43,46,47] For example, different sets of gene expression are induced between the pulsatile and sustained activation of Erk signaling in rat kidney epithelial cells: pulsatile Erk activation preferentially up-regulates the expression of genes under the control of serum response factor, while sustained Erk activation up-regulates genes under the control of AP1 and TEF1.[38] Another example is luteinizing hormone-releasing hormone (LHRH). When LHRH is secreted into the bloodstream in a pulsatile manner, it stimulates the secretion of LH or follicle-stimulating hormone (FSH).[48,49,50] However, the continuous administration of LHRH inhibits LH and FSH secretion because the LHRH receptor is desensitized rapidly.[50,51] Thus, LHRH can display opposing functions depending on its pulsatile or continuous secretion patterns. These results raised an interesting common feature that oscillatory versus sustained expression dynamics of single factors lead to different outcomes in many biological events.

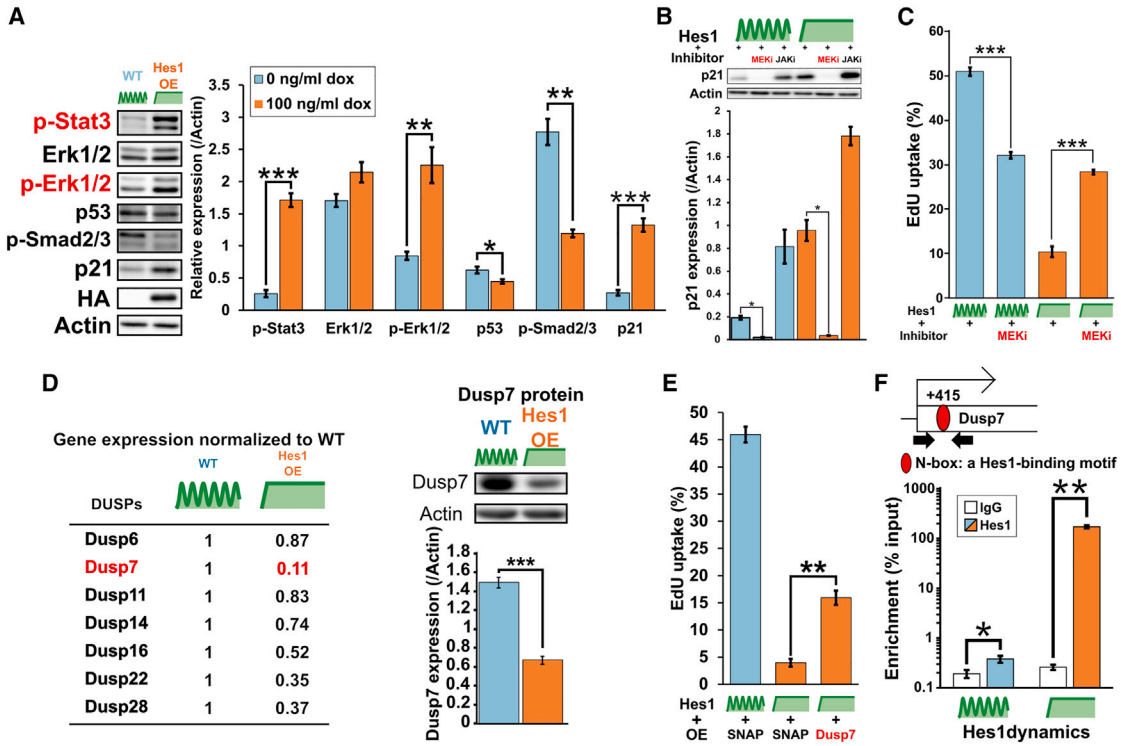

Figure 4. p21 up-regulation in NSCs by sustained Hes1 overexpression via the MEK-Erk signaling

(A) Changes in the expression levels by sustained Hes1 overexpression compared with the WT. NSCs were treated with Dox (0 or 100 ng/mL) for 24 h. n = 3 independent experiments.

(B) p21 expression in WT and *Hes1*-OE NSCs with or without MEK/JAK inhibitors. NSCs were treated with Dox (0 or 100 ng/mL) and inhibitors (MEKi, 100 nM PD0325901; JAKi, 10 μM AG490) for 24 h. n = 3 independent experiments.

(C) EdU incorporation in *Hes1*-OE NSCs with or without a MEK inhibitor. NSCs were treated with Dox (0 or 100 ng/mL) and 100 nM PD0325901 for 2 days. n = 6 independent experiments.

(D) Fold changes of Dusp expression by high and sustained Hes1 expression. (Left table) Expression levels of Dusps were compared between WT and *Hes1*-OE NSCs. (Right figure and graph) Dusp7 protein expression was compared between WT and *Hes1*-OE NSCs. n = 6 independent experiments.

(E) EdU incorporation of *Hes1*-OE NSCs with or without Dusp7 induction. n = 3 independent experiments.

(F) Chromatin immunoprecipitation qPCR with an anti-Hes1 antibody or control IgG on the regulatory sequence in the Dusp7 gene. Chromatin was isolated from WT NSCs or NSCs at 24 h after *Hes1* overexpression induced by the Tet-ON system with 100 ng/mL Dox. qPCR analysis was performed with primers for the binding sites shown in the schematic. n = 3 independent experiments.

Data represent means ± SEM (*p < 0.05, **p < 0.01, ***p < 0.001; Student's t test). See the raw data in Figure S4.

Limitations of the study

Previously, we showed that in the absence of *Hes1*, *Hes3*, *Hes5*, and *Hey1*, all NSCs differentiate prematurely into neurons and are depleted in the mouse embryo and adult nervous system.[8] Furthermore, sustained Hes1 overexpression can induce quiescence in NSCs in the adult brain.[8] However, in our culture condition using epidermal growth factor (EGF) and basic fibroblast growth factor (bFGF), even *Hes1*;*Hes3*;*Hes5*;*Hey1*-KO NSCs could still proliferate, and sustained Hes1 overexpression can slow down the proliferation of cultured NSCs but cannot induce their quiescence. Thus, our culture condition is prone to proliferation and may override the essential roles of the Notch-Hes signaling pathway, leading to an underestimation of the effect of Hes1 on NSC proliferation. More neutral culture conditions would be preferable to investigate the role of Hes1 in NSC quiescence.

Another issue is that p21 expression in the isthmus depends on high and sustained Hes1 expression, but not all quiescent NSCs express high levels of p21. For example, quiescent NSCs in the developing telencephalon, which later become adult NSCs, express high levels of the CDK inhibitor p57 and Hey1.[51,52] These results suggest that different CDK inhibitors may be responsible for NSC quiescence depending on different Hes/Hey members, but it remains to be analyzed whether the expression of other CDK inhibitors also depends on p-Erk1/2 signaling.

STAR★METHODS

Detailed methods are provided in the online version of this paper and include the following:

- KEY RESOURCES TABLE
- RESOURCE AVAILABILITY
  - Lead contact
  - Materials availability
  - Data and code availability

SUPPLEMENTAL INFORMATION

Supplemental information can be found online at https://doi.org/10.1016/j.celrep.2023.112520.

ACKNOWLEDGMENTS

We thank Austin Smith for NS5 cells, Atsushi Miyawaki for the FUCCI probe, Michael Lin for Clover, Feng Zhang for eSpCas9(1.1), Daisuke Asanuma for the HaloTag (SiR700/JF646) ligand, Didier Trono for psPAX2 and pMD2.G, and the RIKEN CBS-EVIDENT Open Collaboration Center for technical support. This work was supported by the Core Research for Evolutional Science and Technology (JP21gm1110002 to R.K.) from the Japan Agency for Medical Research and Development (AMED), Precursory Research for Embryonic Science and Technology (JPMJPR2043 to A.I.) from the Japan Science and Technology Agency (JST), and Specially Promoted Research (21H04976 to R.K.) from the Ministry of Education, Culture, Sports, Science, and Technology (MEXT), Japan.

AUTHOR CONTRIBUTIONS

Y.M. performed the experiments, analyzed the data, and wrote the manuscript; A.I. made p21-luc and analyzed the data; T.M. performed cell culture experiments; R.K. designed and supervised the project and wrote the manuscript.

DECLARATION OF INTERESTS

The authors declare no competing interests.

Received: June 23, 2022
Revised: January 6, 2023
Accepted: May 2, 2023
Published: May 17, 2023

REFERENCES

1. Urbán, N., Blomfield, I.M., and Guillemot, F. (2019). Quiescence of adult mammalian neural stem cells: a highly regulated rest. Neuron *104*, 834–848. https://doi.org/10.1016/j.neuron.2019.09.026.
2. Nyfeler, Y., Kirch, R.D., Mantei, N., Leone, D.P., Radtke, F., Suter, U., and Taylor, V. (2005). Jagged1 signals in the postnatal subventricular zone are required for neural stem cell self-renewal. EMBO J. *24*, 3504–3515. https://doi.org/10.1038/sj.emboj.7600816.
3. Ables, J.L., Decarolis, N.A., Johnson, M.A., Rivera, P.D., Gao, Z., Cooper, D.C., Radtke, F., Hsieh, J., and Eisch, A.,J. (2010). Notch1 is required for maintenance of the reservoir of adult hippocampal stem cells. J. Neurosci. *30*, 10484–10492. https://doi.org/10.1523/JNEUROSCI.4721-09.2010.
4. Ehm, O., Göritz, C., Covic, M., Schäffner, I., Schwarz, T.J., Karaca, E., Kempkes, B., Kremmer, E., Pfrieger, F.W., Espinosa, L., et al. (2010). RBPJF0EA-dependent signaling is essential for long-term maintenance of neural stem cells in the adult hippocampus. J. Neurosci. *30*, 13794–13807. https://doi.org/10.1523/JNEUROSCI.1567-10.2010.
5. Imayoshi, I., Sakamoto, M., Yamaguchi, M., Mori, K., and Kageyama, R. (2010). Essential roles of Notch signaling in maintenance of neural stem cells in the developing and adult brains. J. Neurosci. *30*, 3489–3498. https://doi.org/10.1523/JNEUROSCI.4987-09.2010.
6. Basak, O., Giachino, C., Fiorini, E., Macdonald, H.R., and Taylor, V. (2012). Neurogenic subventricular zone stem/progenitor cells are Notch1-dependent in their active but not quiescent state. J. Neurosci. *32*, 5654–5666. https://doi.org/10.1523/JNEUROSCI.0455-12.2012.
7. Engler, A., Rolando, C., Giachino, C., Saotome, I., Erni, A., Brien, C., Zhang, R., ZimberStrobl, U., Radtke, F., Artavanis-Tsakonas, S., et al. (2018). Notch2 signaling maintains NSC quiescence in the murine ventricular-subventricular zone. Cell Rep. *22*, 992–1002. https://doi.org/10.1016/j.celrep.2017.12.094.
8. Sueda, R., Imayoshi, I., Harima, Y., and Kageyama, R. (2019). High Hes1 expression and resultant Ascl1 suppression regulate quiescent versus active neural stem cells in the adult mouse brain. Genes Dev. *33*, 511–523. https://doi.org/10.1101/gad.323196.118.
9. Imayoshi, I., Isomura, A., Harima, Y., Kawaguchi, K., Kori, H., Miyachi, H., Fujiwara, T., Ishidate, F., and Kageyama, R. (2013). Oscillatory control of factors determining multipotency and fate in mouse neural progenitors. Science *342*, 1203–1208. https://doi.org/10.1126/science.1242366.
10. Shimojo, H., Isomura, A., Ohtsuka, T., Kori, H., Miyachi, H., and Kageyama, R. (2016). Oscillatory control of Delta-like1 in cell interactions regulates dynamic gene expression and tissue morphogenesis. Genes Dev. *30*, 102–116. https://doi.org/10.1101/gad.270785.115.
11. Ochi, S., Imaizumi, Y., Shimojo, H., Miyachi, H., and Kageyama, R. (2020). Oscillatory expression of Hes1 regulates cell proliferation and neuronal differentiation in the embryonic brain. Development *147*, dev182204. https://doi.org/10.1242/dev.182204.
12. Hirata, H., Tomita, K., Bessho, Y., and Kageyama, R. (2001). *Hes1* and *Hes3* regulate maintenance of the isthmic organizer and development of the mid/hindbrain. EMBO J. *20*, 4454–4466. https://doi.org/10.1093/emboj/20.16.4454.
13. Baek, J.H., Hatakeyama, J., Sakamoto, S., Ohtsuka, T., and Kageyama, R. (2006). Persistent and high levels of Hes1 expression regulate boundary formation in the developing central nervous system. Development *133*, 2467–2476. https://doi.org/10.1242/dev.02403.
14. Yoshiura, S., Ohtsuka, T., Takenaka, Y., Nagahara, H., Yoshikawa, K., and Kageyama, R. (2007). Ultradian oscillations in Stat, Smad and Hes1 expression in response to serum. Proc. Natl. Acad. Sci. USA *104*, 11292–11297. https://doi.org/10.1073/pnas.0701837104.
15. Sang, L., Coller, H.A., and Roberts, J.M. (2008). Control of the reversibility of cellular quiescence by the transcriptional repressor HES1. Science *321*, 1095–1100. https://doi.org/10.1126/science.1155998.
16. Noda, N., Honma, S., and Ohmiya, Y. (2011). Hes1 is required for contact inhibition of cell proliferation in 3T3-L1 preadipocytes. Gene Cell. *16*, 704–713. https://doi.org/10.1111/j.1365-2443.2011.01518.x.
17. Yu, X., Alder, J.K., Chun, J.H., Friedman, A.D., Heimfeld, S., Cheng, L., and Civin, C.I. (2006). HES1 inhibits cycling of hematopoietic progenitor cells

via DNA binding. Stem Cell. *24*, 876–888. https://doi.org/10.1634/stemcells.2005-0598.

18. Mourikis, P., Sambasivan, R., Castel, D., Rocheteau, P., Bizzarro, V., and Tajbakhsh, S. (2012). A critical requirement for Notch signaling in maintenance of the quiescent skeletal muscle stem cell state. Stem Cell. *30*, 243–252. https://doi.org/10.1002/stem.775.
19. Lahmann, I., Bröhl, D., Zyrianova, T., Isomura, A., Czajkowski, M.T., Kapoor, V., Griger, J., Ruffault, P.-L., Mademtzoglou, D., Zammit, P.S., et al. (2019). Oscillations of Hes1 and MyoD proteins regulate the maintenance of activated muscle stem cells. Genes Dev. *33*, 524–535. https://doi.org/10.1101/gad.322818.118.
20. Abbas, T., and Dutta, A. (2009). p21 in cancer: intricate networks and multiple activities. Nat. Rev. Cancer *9*, 400–414. https://doi.org/10.1038/nrc2657.
21. LaBaer, J., Garrett, M.D., Stevenson, L.F., Slingerland, J.M., Sandhu, C., Chou, H.S., Fattaey, A., and Harlow, E. (1997). New functional activities for the p21 family of CDK inhibitors. Genes Dev. *11*, 847–862. https://doi.org/10.1101/gad.11.7.847.
22. Sakaue-Sawano, A., Yo, M., Komatsu, N., Hiratsuka, T., Kogure, T., Hoshida, T., Goshima, N., Matsuda, M., Miyoshi, H., and Miyawaki, A. (2017). Genetically encoded tools for optical dissection of the mammalian cell cycle. Mol. Cell *68*, 626–640.e5. https://doi.org/10.1016/j.molcel.2017.10.001.
23. Pollard, S.M., Conti, L., Sun, Y., Goffredo, D., and Smith, A. (2006). Adherent neural stem (NS) cells from fetal and adult forebrain. Cerebr. Cortex *16*, i112–i120. https://doi.org/10.1093/cercor/bhj167.
24. Isomura, A., Ogushi, F., Kori, H., and Kageyama, R. (2017). Optogenetic perturbation and bioluminescence imaging to analyze cell-to-cell transfer of oscillatory information. Genes Dev. *31*, 524–535. https://doi.org/10.1101/gad.294546.116.
25. Festuccia, N., Gonzalez, I., Owens, N., and Navarro, P. (2017). Mototic bookmarking in development and stem cells. Development *144*, 3633–3645. https://doi.org/10.1242/dev.146522.
26. Palozola, K.C., Lerner, J., and Zaret, K.S. (2019). A changing paradigm of transcriptional memory propagation through mitosis. Nat. Rev. Mol. Cell Biol. *20*, 55–64. https://doi.org/10.1038/s41580-018-0077-z.
27. Sabherwal, N., Rowntree, A., Marinopoulou, E., Pettini, T., Hourihane, S., Thomas, R., Soto, X., Kursawe, J., and Papalopulu, N. (2021). Differential phase register of Hes1 oscillations with mitoses underlies cell-cycle heterogeneity in ER^+ breast cancer cell. Proc. Natl. Acad. Sci. USA *118*, e2113527118. https://doi.org/10.1073/pnas.2113527118.
28. Hatakeyama, J., Bessho, Y., Katoh, K., Ookawara, S., Fujioka, M., Guillemot, F., and Kageyama, R. (2004). *Hes* genes regulate size, shape and histogenesis of the nervous system by control of the timing of neural stem cell differentiation. Development *131*, 5539–5550. https://doi.org/10.1242/dev.01436.
29. Trokovic, R., Jukkola, T., Saarimäki, J., Peltopuro, P., Naserke, T., Weisenhorn, D.M.V., Trokovic, N., Wurst, W., and Partanen, J. (2005). Fgfr1-dependent boundary cells between developing mid- and hindbrain. Dev. Biol. *278*, 428–439. https://doi.org/10.1016/j.ydbio.2004.11.024.
30. Hafner, A., Reyes, J., Stewart-Ornstein, J., Tsabar, M., Jambhekar, A., and Lahav, G. (2020). Quantifying the central dogma in the p53 pathway in live single cells. Cell Syst. *10*, 495–505.e4. https://doi.org/10.1016/j.cels.2020.05.001.
31. Nishitani, H., Shiomi, Y., Iida, H., Michishita, M., Takami, T., and Tsurimoto, T. (2008). CDK inhibitor p21 is degraded by a proliferating cell nuclear antigen-coupled Cul4-$DDB1^{Cdt2}$ pathway during S phase and after UV irradiation. J. Biol. Chem. *283*, 29045–29052. https://doi.org/10.1074/jbc.M806045200.
32. Hsu, C.-H., Altschuler, S.J., and Wu, L.F. (2019). Patterns of early p21 dynamics determine proliferation-senescence cell fate after chemotherapy. Cell *178*, 361–373.e12. https://doi.org/10.1016/j.cell.2019.05.041.
33. Yoshioka-Kobayashi, K., Matsumiya, M., Niino, Y., Isomura, A., Kori, H., Miyawaki, A., and Kageyama, R. (2020). Coupling delay controls synchronized oscillation in the segmentation clock. Nature *580*, 119–123. https://doi.org/10.1038/s41586-019-1882-z.
34. Sasai, Y., Kageyama, R., Tagawa, Y., Shigemoto, R., and Nakanishi, S. (1992). Two mammalian helix-loop-helix factors structurally related to *Drosophila hairy* and *Enhancer of split*. Genes Dev. *6*, 2620–2634. https://doi.org/10.1101/gad.6.12b.2620.
35. Ju, B.G., Solum, D., Song, E.J., Lee, K.J., Rose, D.W., Glass, C.K., and Rosenfeld, M.G. (2004). Activating the PARP-1 sensor component of the groucho/TLE1 corepressor complex mediates a CaMKinase IIdelta-dependent neurogenic gene activation pathway. Cell *119*, 815–829. https://doi.org/10.1016/j.cell.2004.11.017.
36. Sugita, S., Hosaka, Y., Okada, K., Mori, D., Yano, F., Kobayashi, H., Taniguchi, Y., Mori, Y., Okuma, T., Chang, S.H., et al. (2015). Transcription factor Hes1 modulates osteoarthritis development in cooperation with calcium/calmodulin-dependent protein kinase 2. Proc. Natl. Acad. Sci. USA *112*, 3080–3085. https://doi.org/10.1073/pnas.1419699112.
37. Albeck, J.G., Mills, G.B., and Brugge, J.S. (2013). Frequency-modulated pulses of ERK activity transmit quantitative proliferation signals. Mol. Cell *49*, 249–261. https://doi.org/10.1016/j.molcel.2012.11.002.
38. Aoki, K., Kumagai, Y., Sakurai, A., Komatsu, N., Fujita, Y., Shionyu, C., and Matsuda, M. (2013). Stochastic ERK activation induced by noise and cell-to-cell propagation regulates cell density-dependent proliferation. Mol. Cell *52*, 529–540. https://doi.org/10.1016/j.molcel.2013.09.015.
39. Pumiglia, K.M., and Decker, S.J. (1997). Cell cycle arrest mediated by the MEK/mitogen-activated protein kinase pathway. Proc. Natl. Acad. Sci. USA *94*, 448–452. https://doi.org/10.1073/pnas.94.2.448.
40. Kerkhoff, E., and Rapp, U.R. (1998). Cell cycle targets of Ras/Raf signalling. Oncogene *17*, 1457–1462. https://doi.org/10.1038/sj.onc.1202185.
41. Regot, S., Hughey, J.J., Bajar, B.T., Carrasco, S., and Covert, M.W. (2014). High-sensitivity measurements of multiple kinase activities in live single cells. Cell *157*, 1724–1734. https://doi.org/10.1016/j.cell.2014.04.039.
42. Marinopoulou, E., Biga, V., Sabherwal, N., Miller, A., Desai, J., Adamson, A.D., and Papalopulu, N. (2021). HES1 protein oscillations are necessary for neural stem cells to exit from quiescence. iScience *24*, 103198. https://doi.org/10.1016/j.isci.2021.103198.
43. Levine, J.H., Lin, Y., and Elowitz, M.B. (2013). Functional roles of pulsing in genetic circuits. Science *342*, 1193–1200. https://doi.org/10.1126/science.1239999.
44. Castro, D.S., Martynoga, B., Parras, C., Ramesh, V., Pacary, E., Johnston, C., Drechsel, D., Lebel-Potter, M., Garcia, L.G., Hunt, C., et al. (2011). A novel function of the proneural gene Ascl1 in progenitor proliferation identified by genome-wide characterization of its targets. Genes Dev. *25*, 930–945. https://doi.org/10.1101/gad.627811.
45. Shimojo, H., Ohtsuka, T., and Kageyama, R. (2008). Oscillations in Notch signaling regulate maintenance of neural progenitors. Neuron *58*, 52–64. https://doi.org/10.1016/j.neuron.2008.02.014.
46. Purvis, J.E., and Lahav, G. (2013). Encoding and decoding cellular information through signaling dynamics. Cell *152*, 945–956. https://doi.org/10.1016/j.cell.2013.02.005.
47. Isomura, A., and Kageyama, R. (2014). Ultradian oscillators: rhythms and cell fate decisions. Development *141*, 3627–3636. https://doi.org/10.1242/dev.104497.
48. Belchetz, P.E., Plant, T.M., Nakai, Y., Keogh, E.J., and Knobil, E. (1978). Hypophysial responses to continuous and intermittent delivery of hypothalamic gonadotropin-relaeasing hormone. Science *202*, 631–633. https://doi.org/10.1126/science.100883.
49. Wildt, L., Häusler, A., Marshall, G., Hutchison, J.S., Plant, T.M., Belchetz, P.E., and Knobil, E. (1981). Frequency and amplitude of gonado-tropin releasing hormone stimulation and gonadotropin secretion in the rhesus monkey. Endocrinology *109*, 376–385. https://doi.org/10.1210/endo-109-2-376.
50. Kobayashi, T., Mizuno, H., Imayoshi, I., Furusawa, C., Shirahige, K., and Kageyama, R. (2009). The cyclic gene *Hes1* contributes to diverse

differentiation responses of embryonic stem cells. Genes Dev. *23*, 1870–1875. https://doi.org/10.1101/gad.1823109.

51. Furutachi, S., Miya, H., Watanabe, T., Kawai, H., Yamasaki, N., Harada, Y., Imayoshi, I., Nelson, M., Nakayama, K.I., Hirabayashi, Y., and Gotoh, Y. (2015). Slowly dividing neural progenitors are an embryonic origin of adult neural stem cells. Nat. Neurosci. *18*, 657–665. https://doi.org/10.1038/nn.3989.
52. Harada, Y., Yamada, M., Imayoshi, I., Kageyama, R., Suzuki, Y., Kuniya, T., Furutachi, S., Kawaguchi, D., and Gotoh, Y. (2021). Cell cycle arrest determines adult neural stem cell ontogeny by an embryonic Notch-nonoscillatory *Hey1* module. Nat. Commun. *12*, 6562. https://doi.org/10.1038/s41467-021-26605-0.
53. Kaise, T., Fukui, M., Sueda, R., Piao, W., Yamada, M., Kobayashi, T., Imayoshi, I., and Kageyama, R. (2022). Functional rejuvenation of aged neural stem cells by Plagl2 and anti-Dyrk1a activity. Genes Dev. *36*, 23–37. https://doi.org/10.1101/gad.349000.121.
54. Slaymaker, I.M., Gao, L., Zetsche, B., Scott, D.A., Yan, W.X., and Zhang, F. (2016). Rationally engineered Cas9 nucleases with improved specificity. Science *351*, 84–88. https://doi.org/10.1126/science.aad5227.
55. Miyoshi, H. (2004). Gene delivery to hematopoietic stem cells using lentiviral vectors. Methods Mol. Biol. *246*, 429–438. https://doi.org/10.1385/1-59259-650-9:429.
56. Lam, A.J., St-Pierre, F., Gong, Y., Marshall, J.D., Cranfill, P.J., Baird, M.A., McKeown, M.R., Wiedenmann, J., Davidson, M.W., Schnitzer, M.J., et al. (2012). Improving FRET dynamic range with bright green and red fluorescent proteins. Nat. Methods *9*, 1005–1012. https://doi.org/10.1038/nmeth.2171.
57. Schindelin, J., Arganda-Carreras, I., Frise, E., Kaynig, V., Longair, M., Pietzsch, T., Preibisch, S., Rueden, C., Saalfeld, S., Schmid, B., et al. (2012). Fiji: an open-source platform for biological-image analysis. Nat. Methods *9*, 676–682. https://doi.org/10.1038/nmeth.2019.
58. Tinevez, J.Y., Perry, N., Schindelin, J., Hoopes, G.M., Reynolds, G.D., Laplantine, E., Bednarek, S.Y., Shorte, S.L., and Eliceiri, K.W. (2017). TrackMate: an open and extensible platform for single-particle tracking. Methods *115*, 80–90. https://doi.org/10.1016/j.ymeth.2016.09.016.
59. Kawakami, K. (2007). Tol2: a versatile gene transfer vector in vertebrates. Genome Biol. *8*, S7. https://doi.org/10.1186/gb-2007-8-s1-s7.
60. Yagita, K., Yamanaka, I., Emoto, N., Kawakami, K., and Shimada, S. (2010). Real-time monitoring of circadian clock oscillations in primary cultures of mammalian cells using Tol2 transposon-mediated gene transfer strategy. BMC Biotechnol. *10*, 3. https://doi.org/10.1186/1472-6750-10-3.
61. Mefferd, A.L., Kornepati, A.V.R., Bogerd, H.P., Kennedy, E.M., and Cullen, B.R. (2015). Expression of CRISPR/Cas single guide RNAs using small tRNA promoters. RNA *21*, 1683–1689. https://doi.org/10.1261/rna.051631.115.
62. Shen, M.W., Arbab, M., Hsu, J.Y., Worstell, D., Culbertson, S.J., Krabbe, O., Cassa, C.A., Liu, D.R., Gifford, D.K., and Sherwood, R.I. (2018). Predictable and precise template-free CRISPR editing of pathogenic variants. Nature *563*, 646–651. https://doi.org/10.1038/s41586-018-0686-x.
63. Concordet, J.P., and Haeussler, M. (2018). CRISPOR: intuitive guide selection for CRISPR/Cas9 genome editing experiments and screens. Nucleic Acids Res. *46*, W242–W245. https://doi.org/10.1093/nar/gky354.
64. Kobayashi, T., Piao, W., Takamura, T., Kori, H., Miyachi, H., Kitano, S., Iwamoto, Y., Yamada, M., Imayoshi, I., Shioda, S., et al. (2019). Enhanced lysosomal degradation maintains the quiescent state of neural stem cells. Nat. Commun. *10*, 5446. https://doi.org/10.1038/s41467-019-13203-4.
65. Fellmann, C., Hoffmann, T., Sridhar, V., Hopfgartner, B., Muhar, M., Roth, M., Lai, D.Y., Barbosa, I.A.M., Kwon, J.S., Guan, Y., et al. (2013). An optimized microRNA backbone for effective single-copy RNAi. Cell Rep. *5*, 1704–1713. https://doi.org/10.1016/j.celrep.2013.11.020.

STAR★METHODS

KEY RESOURCES TABLE

REAGENT or RESOURCE	SOURCE	IDENTIFIER
Antibodies		
Rabbit polyclonal anti-Actin	Sigma-Aldrich	Cat# A2066; RRID: AB_476693
Mouse monoclonal anti-p21	Santa Cruz Biotechnology	Cat# sc-6246; RRID: AB_628073
Mouse monoclonal anti-p15/p16	Santa Cruz Biotechnology	Cat# sc-377412; RRID: AB_2936231
Rabbit polyclonal anti-phospho-Stat3 (Tyr705)	Cell Signaling Technology	Cat# 9131; RRID: AB_331586
Rabbit polyclonal anti-Erk1/2	Cell Signaling Technology	Cat# 9102; RRID: AB_330744
Rabbit monoclonal anti-phospho-Erk1/2 (Thr202/Tyr204)	Cell Signaling Technology	Cat# 4377; RRID: AB_331775
Mouse monoclonal anti-p53	Santa Cruz Biotechnology	Cat# sc-126; RRID: AB_628082
Mouse monoclonal anti-phospho-smad3 (Ser 425)	Santa Cruz Biotechnology	Cat# sc-517575; RRID: AB_2892229
Rat monoclonal anti-HA	Sigma-Aldrich	Cat# 11867423001; RRID: AB_390918
Mouse monoclonal anti-PYST2 (Dusp7)	Santa Cruz Biotechnology	Cat# sc-377106; RRID: AB_2936232
Rabbit monoclonal anti-a-Actinin	Cell Signaling Technology	Cat# 6487; RRID: AB_11179206
Rabbit monoclonal anti-HES1	Cell Signaling Technology	Cat# 11988; RRID: AB_2728766
Rabbit polyclonal anti-HES1	Kobayashi et al.[50]	N/A
Normal rabbit IgG	Cell Signaling Technology	Cat# 2729; RRID: AB_1031062
HRP-linked Sheep anti-mouse IgG	Cytiva	Cat# NA9310; RRID: AB_772193
HRP-linked Goat anti-rat IgG	Cytiva	Cat# NA935; RRID: AB_772207
HRP-linked Donkey anti-rabbit IgG	Cytiva	Cat# NA9340; RRID: AB_772191
Bacterial and virus strains		
CSII-EF-Halo-hCdt1 (1/100)Cy(−)	This paper	N/A
CSII-EF-SNAP-P2A-Venus-3NLS	This paper	N/A
CSII-EF-Dusp7-P2A-Venus-3NLS	This paper	N/A
CSII-h7SK-sh-control	Kobayashi et al.[50]	N/A
CSII-h7SK-Hes1-sh4	Kobayashi et al.[50]	N/A
CSII-EF-Puro-P2A-ERK KTR-Clover	This paper	N/A
Chemicals, peptides, and recombinant proteins		
m-IgGκ BP-HRP	Santa Cruz Biotechnology	Cat# sc-516102; RRID: AB_2687626
DAPI	Thermo Fisher Scientific	Cat# 62248
5-ethynyl-2′-deoxyuridine (EdU)	Thermo Fisher Scientific	Cat# A10044
Alexa Fluor 488 Azide	Thermo Fisher Scientific	Cat# A10266
Alexa Fluor 647 Azide	Thermo Fisher Scientific	Cat# A10277
HaloTag ligands (SiR700-Halo and JF646-Halo)	Kindly gifted by Daisuke Asanuma	N/A
doxycycline hyclate (Dox)	Sigma-Aldrich	Cat# D9891
PD0325901	FUJIFILM Wako	Cat# 162-25291
AG490	CALBIOCHEM	Cat# 658401
KN-62	Cayman Chemical	Cat# 13318
Cycloheximide (CHX)	Sigma-Aldrich	Cat# C1988
D-luciferin sodium salt	Nacalai Tesque	Cat# 01493-85
ViaFect Transfection Reagent	Promega	Cat# E4981
Polyethylenimine (PEI)	Polysciences	Cat# 24765
Puromycin dihydrochloride	InvivoGen	Cat# ant-pr-1
Blasticidin S Hydrochloride	Thermo Fisher Scientific	Cat# R21001
G418 disulfate	Nacalai Tesque	Cat# 09380-44
Critical commercial assays		
Click-iT EdU Cell Proliferation Kit	Thermo Fisher Scientific	Cat# C10337

(*Continued on next page*)

Continued

REAGENT or RESOURCE	SOURCE	IDENTIFIER
Deposited data		
RNA-seq data	This paper	DRA: DRA015672
Experimental models: Cell lines		
HEK293T	ATCC	Cat# CRL-3216; RRID: CVCL_0063
NS5	Pollard et al.[23]	N/A
Experimental models: Organisms/strains		
Mouse: Hes1; Hes3; Hes5-null	Hatakeyama et al.[28]	N/A
Mouse: Hes1 flox; Hes3; Hes5; Hey1-null	Sueda et al.[8]	N/A
Oligonucleotides		
Primer: ChIP-p21-Forward ttagtccttcccacagttggtc	This paper	N/A
Primer: ChIP-p21-Reverse acctgggctattctcttgtcac	This paper	N/A
Primer: ChIP-Dusp7-Forward gtccctgctgctgctagatt	This paper	N/A
Primer: ChIP-Dusp7-Reverse aggttgatggccgtctcaat	This paper	N/A
shRNA targeting sequence: p21: TTTAAATAACTTT AAGTTTGGA	Kaise et al.[53]	N/A
shRNA targeting sequence: Hes1: GCCAATTTGCC TTTCTCATCC	Kobayashi et al.[50]	N/A
Recombinant DNA		
CRM5-pHes1-Ub-NLS-Luc2-Hes1 3′UTR	Isomura et al.[24]	N/A
p21_promoter-Ub-NLS-Luc2-p21 3′UTR	This paper	N/A
pTRE_3G-HA-Hes1	This paper	N/A
pTRE_3G-miR-E	This paper	N/A
pTRE_3G-HA-Hes1-miR-E	This paper	N/A
pCAG-rtTA2_3G-P2A-Bsd-P2A-NLS-mcherry	This paper	N/A
pCAG-hGAVPO-P2A-Puro-P2A-NLS-mcherry +pUAS-HA-Hes1	This paper	N/A
eSpCas9(1.1)	Slaymaker et al.[54]	Addgene Plasmid #71814; RRID: Addgene_71814
tRNA-pCBh-eSpCas9(1.1)-P2A-EGFP	This paper	N/A
mouse p21-Achilles targeting vector: pBS-HA_left -Achilles-p2a-NeoR-HA_right	This paper	N/A
CSII-EF-MCS	Imayoshi et al.[9] Miyoshi[55]	N/A
CSII-EF-Halo-hCdt1 (1/100) Cy(−)	This paper	N/A
CSII-EF-SNAP-P2A-Venus-3NLS	This paper	N/A
CSII-EF-Dusp7-P2A-Venus-3NLS	This paper	N/A
CSII-h7SK-sh-control	Kobayashi et al.[50]	N/A
CSII-h7SK-Hes1-sh4	Kobayashi et al.[50]	N/A
CSII-EF-Puro-P2A-ERK KTR-Clover	This paper	N/A
psPAX2	Didier Trono Lab	Addgene Plasmid # 12260; RRID: Addgene_12260
pMD2.G	Didier Trono Lab	Addgene Plasmid # 12259; RRID: Addgene_12259
pcDNA3-AKAR2-CR	Lam et al.[56]	Addgene Plasmid # 40255; RRID: Addgene_40255
Software and algorithms		
Fiji	Schindelin et al.[57]	RRID: SCR_002285
TrackMate	Tinevez et al.[58]	N/A

RESOURCE AVAILABILITY

Lead contact

Further information and requests for resources and reagents should be directed to and will be fulfilled by the Lead Contact, Ryoichiro Kageyama (ryoichiro.kageyama@riken.jp).

Materials availability

Newly generated items in the study are available on request from the lead contact with a completed materials transfer agreement.

Data and code availability

- The transcriptome data have been deposited in the DDBJ Sequence Read Archive (DRA) under the accession number DRA015672.
- This paper does not report original code.
- Any additional information required to reanalyze the data reported in this paper is available from the lead contact upon request.

EXPERIMENTAL MODEL AND SUBJECT DETAILS

Animals

Hes1 flox;*Hes3*;*Hes5;Hey1*-null mice were previously described.[8] NSCs were established from E14.5 embryos of these mice. *Hes1*;*Hes3*;*Hes5*-null mice were previously described.[28] E9.5 embryos of these mice were obtained by crossing *Hes1*(+/−);*Hes3*;*Hes5*-null mice with each other. In all experiments, we used both sexes. All mice were maintained on ICR genetic background. Mice were housed in a temperature-controlled environment under a 12-h light and dark cycle, with free access to food and water. All animal experiments were performed according to the Kyoto University Guide for the Care and Use of Laboratory Animals, and animal protocols were approved by the Experimental Animal Committee of the Institute for Frontier Life and Medical Sciences, Kyoto University.

Cell lines and cultures

We cultured HEK293T cells (American Type Culture Collection [ATCC]) in DMEM (Nacalai Tesque, 08458-16) supplemented with 10% fetal bovine serum (FBS; Nichirei Biosciences, 175012) and 100 units/mL penicillin and 100 mg/mL of streptomycin (Nacalai Tesque, 09367-34) in a 5% CO2 incubator at 37°C. Neural stem cells (NSCs) were cultured in growth medium [20 ng/mL EGF (Thermo, 53003-018), 20 ng/mL bFGF (Wako, 060–04543), penicillin/streptomycin, and N-2 Plus Media Supplement (R&D Systems, AR003) in DMEM/F-12 (Gibco, 11039-021)] with 2 μg/mL laminin (Wako, 120–05751) or Matrigel (3:2000, Corning, 356231). Quiescence was induced with quiescent medium [50 ng/mL BMP4 (R&D Systems, 314-BP), 20 ng/mL bFGF, penicillin/streptomycin, and N-2 Plus supplement in DMEM/F-12] after two washings with phosphate-buffered saline (PBS; Nacalai Tesque).

NS5 cell line was derived from mouse ES cells (a kind gift from A. Smith).[23] Embryo-derived NSCs were established from mouse embryos at E14.5. These NSCs were frozen several times and then passed at least ten times before use. *Hes3*;*Hes5*;*Hey1*-KO NSCs were established from *Hes1* flox;*Hes3*;*Hes5*;*Hey1*-null mouse embryos at E14.5. *Hes1*;*Hes3*;*Hes5*;*Hey1*-KO NSCs were generated by expressing Cre recombinase in *Hes1* flox;*Hes3*;*Hes5*;*Hey1*-null NSCs.

METHOD DETAILS

Plasmid construction

We used standard molecular biology techniques to make the constructs. Most plasmids were based on the Tol2 transposon vector system, a gift from K. Kawakami.[59,60] The Hes1 promoter reporter consisted of the Hes1 cis-regulatory motif (CRM5), the Hes1 promoter region (−2567 to +223), Ub-NLS-Luc2 reporter and Hes1 3′UTR, as previously described.[24] The p21 promoter reporter consisted of p21 promoter region (−5248 to +93), Ub-NLS-Luc2 reporter, p21 3′UTR. Tet-ON system consisted of rtTA_3G and NLS-mCherry and Bsd driven by CAG promoter and TRE_3G promoter inducing genes and miR-E. In this article, we induced HA-Hes1, miR-E and HA-Hes1-miR-E.

The following sequences were used for knockdown.

p21: TTTAAATAACTTTAAGTTTGGA.

Hes1: GCCAATTTGCCTTTCTCATCC.

As a negative control, scramble sequences were used. The light-inducible expression system consisted of hGAVPO and NLS-mCherry and Puro driven by CAG promoter and HA-tagged Hes1 driven by UAS promoter.[24] As a negative control, only hGAVPO driven by CAG promoter was used.

To make eSpCas9 (1.1) expression vector, we modified "eSpCas9(1.1)" (Addgene, #71814). This vector expressed eSpCas9 (1.1)-P2A-EGFP driven by CBh promoter and sgRNA driven by Glutamine tRNA.[61]

We decided the guide sequence using these two websites, "inDelphi" (https://indelphi.giffordlab.mit.edu/gene)[62] and "CRISPOR" (http://crispor.tefor.net/).[63] The guide sequence used was ggggctcccgtgggcacttca.

In mouse p21-Achilles targeting vector, homology arms (left: 846 bp, right: 820 bp) were tethered to Achilles-P2A-NeoR. The 10 amino acids Glycine-Alanine linker was inserted into C-terminus of p21 and Achilles.

To make lentivirus vectors, we inserted HaloTag, a self-labeling protein tag, fused to N-terminus of hCdt1 (1/100) Cy (−), (SNAP-tag or Dusp7)-P2A-Venus-3NLS and Puro-P2A-ERK KTR-Clover into CSII-EF-MCS.[9,55] For cloning Clover, we used pcDNA3-AKAR2-CR (Addgene Plasmid # 40255).

Production of lentiviruses

Lentiviral particles were produced as follows.[9,55] 8.4 μg of CSII-pEF plasmid, 6.2 μg of second generation lentiviral packaging plasmid (psPAX2, Addgene Plasmid # 12260) and 2.6 μg of VSV-G envelope expressing plasmid (pMD2.G, Addgene Plasmid # 12259) were transfected into HEK293T cells in a 10-cm dish using 86 μL of 1 μg/μL Polyethylenimine (Polysciences). The medium was collected 2 days later and concentrated into phosphate-buffered saline (PBS) at 1/250 of the original volume by centrifugation at 6,000 g for 16 h and 13,000g for 4 h.

Generation of stable cell lines

To establish stable cell lines by Tol2 transposon vector system, NS5 cells were cultured in a 48-well plate with 4×10^4 cell-density and 1 day later, 0.5 μg DNA including 0.1 μg pCAGGS-mT2TP plasmids were transfected using ViaFect Transfection Reagent (Promega). Transfected cells were expanded and drug-selected with either 1 μg/mL Puromycin or 20 μg/mL Blasticidin. Stably transfected cells, which were mCherry- or mTagBFP2-positive, were collected by FACS and, if needed, clonal lines were picked from single isolated colonies.

To establish stable cell lines by lentivirus, NS5 cells were cultured in a 48-well plate with 4×10^4 cell-density and 1 day later, infected with the lentivirus [CSII-EF-Halo-hCdt1 (1/100) Cy(−), CSII-EF-Puro-P2A-ERK KTR-Clover, (SNAP or Dusp7)-P2A-Venus-3NLS]. In the case of CSII-EF-Halo-hCdt1 (1/100) Cy(−), we added 3 μl lentivirus. More than 1 week after infection, we added 1 nM HaloTag ligands and after 30-min incubation, HaloTag-positive cells were collected by FACS. If needed, clonal lines were picked from single isolated colonies. In the case of CSII-EF-Puro-P2A-ERK KTR-Clover, we added 3 μL lentivirus and infected cells were expanded and drug-selected with 1 μg/mL Puromycin. We used infected cells at least 1week after drug selection. In the case of CSII-EF-(SNAP or Dusp7)-P2A-Venus-3NLS, we added 32 μL lentivirus. We used infected cells within 1 week for several experiments.

Achilles knock-in to c-terminus of p21

NS5 cell line cultured in 6-cm dish with 8×10^5 cell-density and 1 day later, 5 μg targeting vector and 5 μg Glu_tRNA-sgRNA-pCBh-eSpCas9 (1.1)-P2A-EGFP were transfected using ViaFect Transfection Reagent (Promega). 2 days later, EGFP-positive cells were collected by FACS. About a week after transfection, we started G418 selection (100 μg/mL). After selection, clonal lines were picked from single isolated colonies. We checked whether knock-in was succeeded by sequencing the genome.

Cell proliferation assay

10 μM of EdU was added, and after 30-min incubation, cells were fixed with 4% PFA for immunocytochemical analysis. Click-iT EdU Cell Proliferation Kit (Invitrogen) was used to detect EdU incorporation.

Chemical inhibitors

We used PD0325901 (Fujifilm Wako, 162–25291), AG490 (Calbiochem, 658401) and KN-62 (Cayman, 13318) as a MEK inhibitor, a JAK inhibitor and a CaMKII inhibitor, respectively. For measuring the half-lives of p21 or p21-achilles, cells were cultured with 10 ng/mL Cycloheximide (Sigma) to block protein synthesis.

Whole mount *in situ* hybridization

Preparation of a DIG-labeled antisense RNA probe and whole-mount *in situ* hybridization using NBT/BCIP (Roche) detection were performed as described previously.[12] p21 (nucleotide residues 250–1176) was used as RNA probes.

Western blot analysis

Western blot was performed as previously described.[64] The amount of each protein band relative to that of actin or actinin band was quantified. The following primary antibodies were used for western blotting: rabbit anti-Actin (Sigma, A2066), mouse anti-p21 (Santa Cruz, sc-6246), mouse anti-p15/16 (Santa Cruz, sc-377412), rabbit ant-p-stat3 (CST, 9131), rabbit anti-Erk1/2 (CST, 9102), rabbit anti-p-Erk1/2 (CST, 4376), mouse anti-p53 (Santa Cruz, sc-126), mouse anti-p-smad3 (Santa Cruz, sc-517575), rat anti-HA (Sigma, 11867423001), mouse anti-Dusp7 (Santa Cruz, sc-377106), rabbit anti-HES1 (CST, 11988) and rabbit anti-a-Actinin (CST, 6487). Secondary antibodies were HRP-conjugated anti-rabbit, mouse, and rat antibodies (GE Healthcare) and HRP-conjugated m-IgGκ binding protein (Santa).

Bioluminescence imaging of NSCs

NS5 cells carrying the Hes1 or p21 promoter reporter[24] and modified Fucci probe[22] were plated into φ27-mm glass-bottom dishes (IWAKI) and cultured with 1 mM luciferin (Nacalai Tesque) and 1 nM SiR700-Halo or JF646-Halo in the growth medium. The dish was placed on the stage of inverted microscope (Olympus IX81 or IX83) and was maintained at 37°C and 5% CO2. Bioluminescence was measured using Olympus objective lens (UPLFLN 40 O) and was transmitted directly to a CCD camera (Andor iKon-M).[9]

Fluorescence imaging of NSCs

Cells were plated into φ27-mm glass-bottom dishes (Iwaki) The dish was placed on the stage of the inverted confocal laser scanning microscope (Olympus FV3000, Zeiss LSM980) and was maintained at 37°C and 5% CO2. Achilles, mCherry, SiR700 were excited

with a 514-nm and 561-nm laser, 633-nm laser respectively. A z stack of images was taken with about 1.4-μm depth intervals every 300s. Fluorescence was measured using object lens (Uplsapo 40xS, 20x).

For p21-Achilles knock-in NS5 cells carrying the modified Fucci probe, we cultured these cells with 1 nM SiR700-Halo in the growth medium and 30 min later, start the imaging by Zeiss LSM980. For measuring the half-life of p21-achilles, we cultured p21-Achilles knock-in NS5 cells in the growth medium. We added Cycloheximide (final: 10 ng/mL) just before starting the imaging by Zeiss LSM980. For ERK KTR-Clover NS5 cells carrying Tet-ON system overexpressing HA-Hes1, we cultured these cells with 0 or 50 ng/mL Dox in the growth medium and start the imaging by Olympus FV3000.

Live cell recording of luminescence signals at the population level

Luminescence signals at the population level were measured by a live cell monitoring system (CL24B-LIC/B, Churitsu Electric Corp.) with a high-sensitive PMT and a LED blue-light source (LEDB-SBOXH, OptoCode). Measurements were done every 5 or 10 min with 5 or 10 s exposures. When light stimulation was performed, we cultured NS5 cells carrying the p21 promoter reporter and light-inducible expression system (hGAVPO+pUAS-HA-Hes1)[24] in the quiescent medium. Blue light was exposed every 3 h with 30 s duration and the intensity of 31.2 W/m^2 measured by a light meter (LI-250A; LI-COR Biosciences).

Sustained overexpression and knockdown controlled by Tet-ON system

Sustained overexpression and knockdown based on miR-E system[65] induced by Tet-ON system. About 1day after plating cells carrying Tet-ON system, we added doxycycline at several concentrations and analyzed these cells 1 or 2 days later.

Chromatin immunoprecipitation (ChIP)-qPCR

ChIP was performed with a rabbit polyclonal anti-HES1 antibody[52] or normal rabbit IgG (CST, 2729). Chromatin was isolated from *Hes1*-overexpressing NSCs 8 or 24 h after a Dox treatment (100 ng/mL). qPCR analysis was performed using the QuantStudio 12K (Life Technologies), Common Use Equipment, in the Support Unit for Bio-Material Analysis, Research Resources Division, RIKEN Center for Brain Science. The detail of primers we used are on the key resources table.

RNA-seq analysis

For comparing gene expression between WT and Hes KO or that between WT and Hes1 overexpression, we collected RNA isolated from WT and *Hes1;Hes3;Hes5;Hey1* KO eNSCs or NS5 carrying Tet-ON systems for overexpressing HA-Hes1 treated with 0 or 100 ng/mL Dox for 1 day, respectively. Triplicates of total RNA samples were isolated from NSCs by NucleoSpin RNA kit (Takara). RNA quality was assessed by RNA Bioanalyzer, confirming that RNA integrity number (RIN) of all samples were above 9. The sequencing libraries were prepared using the NEB Next Ultra II Directional RNA Library Prep Kit for Illumina (NEB). 1 x 75 single-end sequencing was performed by NextSeq 500 (mid-output single-end 75 cycles [Illumina]). cDNA sequences were aligned to the mouse reference genome mm10 by TopHat and counted by Cufflinks. We used Cuffdiff for finding differentially expressed genes ($q < 0.01$). From genes with FPKM>10 that are up-regulated or down-regulated by Hes KO and Hes1 overexpression (Table S1), genes involved in cell cycle regulation were examined using GO term "regulation of cell cycle G1/S phase transition" (GO:1902806).

QUANTIFICATION AND STATISTICAL ANALYSIS

Image processing and time-series analysis

Images were processed by Fiji image analysis software as follows.[24] In the case of bioluminescence, stack images were applied to the Spike Noise Filter (ImageJ plugin) for removing signals from cosmic rays and then to the Savitzky Golay Temporal Filter (ImageJ plugin) for getting clear dynamic expression. In the case of z stack of images, Z projection by max intensity was done, and then stack images were applied to the Savitzky Golay Temporal Filter. If needed, Background was removed by Temporal Background Reduction (ImageJ plugin) or Subtract Background (ImageJ command). Fluorescence and bioluminescence of each single cell were quantified by TrackMate (ImageJ plugin). Cell cycle phase are decided, as follows.[22] The timing of G1/S or S/G2 transition were manually decided depended on the Halo-hCdt1 (1/100)Cy(−) signal, which decreased upon entering S phase and emerged when cells enter G2 phase.

For ERK-KTR Clover analysis, we traced cells 16 to 24 h after starting the imaging. We quantified fluorescence in nucleus and cytosol of each cell by TrackMate or manually and calculated the ratio of fluorescence (Cytosol/Nucleus).

Statistical analysis

Data represent means ± s.e.m. The sample sizes, statistical tests, and p values are indicated in the figures and the figure legends. p values were classified as follows: *$p < 0.05$, **$p < 0.01$, ***$p < 0.001$.